MMA Progress Reports

March, 1989

— CONTENTS —

MMA SITE AND CONFIGURATION

The scientific requirements for the MMA include provision for imaging at an angular resolution comparable to that of the Space Telescope, $0\overset{''}{.}1$, at the principal frequency bands of the MMA. This requirement leads us to an array of 3 km maximum extent. Not all MMA observations need this angular resolution, and, hence, not always will the array be so extended. Indeed, the mosaiced images of extended molecular regions, in the disks of external galaxies and in Galactic molecular clouds, will usually be made with the MMA in a densely-packed configuration of diameter no greater than 100 m. Thus the MMA must be reconfigurable, the antennas transportable, and the site big enough, and flat enough, to permit such reconfiguration. The site must also be at high altitude, to realize the sky transparency needed for precision imaging at 200–350 GHz.

Over the past year we have completed a process of sifting through geographical data on potential MMA sites in the U.S. Southwest that satisfy the above criteria. From surveys of topographical maps we established a list, which we believe to be complete, of over fifty sites that are above 9000 feet altitude and South of latitude 36° N. With this starting list we ranked sites in groups depending on elevation, size, access, and environment (density of trees, distance from the nearest town, etc.). We currently have the following four sites in the 'top' group (listed here in no particular order):

- *Springerville, AZ:* This is a large (10 km), high (9200 feet) plateau in the Apache National Forest about 15 miles from Springerville. Access is by a paved state highway.
- *South Park, CO:* Located in a shallow valley 60 miles West of Colorado Springs at 9300 feet altitude, this site is mostly private land. The prime, flat area is approximately 3 km East–West by 6 km North–South; it is bisected by U.S. Highway 24.
- *Alpine, AZ:* As with the Springerville site, this is also located in the Apache National Forest, adjacent to U.S. Highway 666. We have little information on the site, but what we've seen is interesting: altitude 9900 feet, with a flat open area at least 3 km East–West by 5 km North–South.
- *Magdalena Mountains, NM:* This site is on a high (10,500 feet) mountaintop on the grounds of the Langmuir Laboratory Scientific Preserve in Cibola National Forest. The site is irregularly shaped but would accommodate a 3 km MMA configuration.

We have not yet sought permission to use any of these sites; discussions on this issue with the agencies and/or individuals involved have just begun.

We are also looking carefully at an even higher altitude site on Mauna Kea, HI, recognizing that there will be, in this case, a compromise to be reached between the potential gain of greater atmospheric transparency and the loss of the longer MMA baselines, owing to the unfavorable topography of that mountain. Finally, an even more extreme possibility for the MMA site exists in the Southern Hemisphere, in Chile, where it appears possible to find a flat site at very high altitude. The logistics would be formidable and the incremental cost increase of the project could be substantial. We will follow with interest ESO's analysis of these same considerations as they assess southern sites for the VLT.

In Situ Measurements

For two years we have operated a 225 GHz tipping radiometer on the potential MMA site in the Magdalena Mountains. As part of its cycle of operation, this device not only does sky tips to measure the zenith 225 GHz opacity, but once every ten hours it takes an hour of rapidly sampled total-power measurements at the zenith. Tests at the VLA confirm the correlation between the power spectrum of these fluctuations and the variations seen in the VLA interferometer phase. Thus, the 225 GHz fluctuation spectrum can be used to provide an estimate of the interferometer phase expected on a remote site.

Ultimately, the plan is to test each of the most promising sites with one of the radiometers. For each site we hope to obtain a measure of the fraction of time that the atmospheric transparency at the site will permit operation at each of the four principal MMA frequency bands, and from the fluctuation spectrum, the fraction of time at each site during which coherence can be maintained with an interferometer over timescales of a few minutes.

Bob Martin at Steward Observatory has demonstrated the effectiveness of a related technique which permits one to estimate the atmospheric transparency at high frequency, given NOAA radiosonde observations and a good atmospheric model. The advantages of this technique are that one has access to a very extensive radiosonde database, compiled over two decades, which provides a measure of the long-term trends and that one can use to 'site test' in a computer. The disadvantage is that radiosondes are not launched from the site, itself, that one wishes to test. One must assume, *post facto*, that the atmosphere measured some distance from the radiosonde launch site is, in fact, representative also of the sky over the site of interest. In addition, the radiosondes provide no measure of the prospective interferometer coherence time.

We have accumulated the NOAA radiosonde measurements near each of the prospective MMA sites, including those near Mauna Kea (Hilo) and northern Chile (Antofagasta). A preliminary analysis of these data has been made and is available for distribution. The radiosonde data from Albuquerque, NM, are of particular interest to us because we can compare directly the sky transparency over the Magdalena mountains, as inferred from the radiosonde, with our direct *in situ* radiometric measurements. Exceptionally good mean seasonal agreement is seen for the two techniques, but there are noticeable differences in some of the data taken simultaneously. Presumably, this latter disagreement is attributable to local effects. A careful analysis of the radiosonde data for all the prospective MMA sites is in progress. It will be used in conjunction with the radiometer measurements, not instead of the radiometer work, in helping us to characterize each of the potential MMA sites.

MMA ANTENNA AND TELESCOPE OPTICS

Since the 350 GHz atmospheric window is one of the two frequency bands given particular emphasis by the MMA (the other being the 1-mm band, 200–300 GHz) the antennas must permit precision operation at this frequency. The MMA Design Study Volume II had specified a surface accuracy of $\lambda/16$ at the shortest wavelength, 850 microns. However, this implies a 46% reduction in gain, relative to the antenna efficiency at lower frequencies—i.e., a somewhat marginal performance. Tightening the specifications to a 25 micron r.m.s. surface brings the gain reduction down to a little over 10%, which gives the array high performance in this atmospheric window. As a by-product, the array would also have usable performance up to the 500 GHz atmospheric window, but the primary objective in setting this surface specification is to achieve good performance at 350 GHz.

Another critical parameter is the telescope pointing accuracy. In order for mosaicing to be successful, the pointing of each element needs to be good to approximately 1/20 of a beamwidth, or about 1 arcsecond at 1 mm. This aspect is being studied in detail within the Central Element Study Group. The Design Study Volume II had specified 3 arcseconds, but this now appears to be inadequate.

The Working Group on MMA antennas reviewed the existing telescope designs of those few operational antennas that achieve performance similar to the revised MMA specifications. In doing so we discovered that if these tighter specifications are to be realized there are several implications. First, owing to thermal effects, an all-steel antenna design is unlikely to be able to meet the specifications. Incorporating carbon-fiber- reinforced plastic (CFRP) into the design may be appropriate—a route chosen for other successful high-precision antennas (IRAM, SMT). At present, there is little experience within the U.S. in the use of CFRP in antenna construction. The revised specifications would probably make the antennas more costly—and the dominant component in the overall construction cost of the project. During the lifetime of the array, receivers and computers are likely to be replaced as newer technology becomes available, but the antennas themselves are unlikely to be replaced. This suggests that the basic antenna design may provide the ultimate limitation in performance of the array: it would be unfortunate to compromise this at the start with too marginal a design. Experience with the SMT project suggests that the cost equations used to optimize the size and number of antennas may, in any case, need slight revision. However, we do not expect a very dramatic deviation from the current proposal for 30–40 antennas, each 7.5–8.5 m in diameter.

There are various options which could be chosen for the antenna design, e.g., an off-axis feed to reduce sidelobes, and a polar mount so that sidelobes do not rotate on the sky. However, as a starting point a trial antenna concept has been developed for a symmetric on-axis, Az–El antenna using a Coudé focus cabin arrangement. The philosophy behind the design it to achieve a means for bringing the antenna beam to a convenient focus for coupling into the receiver. For reasons of convenience and reliability, the receivers should be mounted in fixed positions within the plinth of the antenna.

Figure 1 illustrates the proposed design. It is a conventional Cassegrain except that the secondary focus is brought right down into the plinth (Coudé focus). The receivers are located in fixed positions in the base of the antenna, a design feature which offers the following advantages:

(1) The receivers are easily accessible;
(2) Telescope balance is not affected by removing or installing receivers;
(3) Effects of cable and compressor line drag on the pointing are eliminated.

Primary Mirror

It is assumed that the diameter D of the primary reflector will be 8.0 m. The primary will be a symmetric paraboloid with a focal length f of 3.2 m, yielding a primary f-ratio (f/D) of 0.4. This value gives a compact antenna. It could be reduced further (to $f/D = 0.35$, say), but the tolerances in locating the secondary are more stringent (both for pointing and for beam quality). The primary mirror requires a central hole to pass the beam from the secondary to the receivers. Its size is determined by the field-of-view and the required secondary focal length. A diameter d_h of 1.0 m is close to optimum.

Secondary Mirror

The secondary mirror will be a symmetric hyperboloid. Its size is set principally by the field-of-view (approximately 10 arcseconds) and the requirement to have the secondary focus in the receiver room. It should be as small as possible, within these constraints, in order to minimize blockage and allow for the possibility of nutation for beam switching at some stage.

A diameter of 800 mm and a distance between foci of 9.79 m gives an effective f-ratio at the secondary focus of 12, which is convenient for most quasi-optical systems. With some more optimization the secondary diameter could be reduced but probably could not be made much less than 750 mm. Similarly, the focal ratio could be changed, but it is fairly tightly constrained and will probably be in the range 11 to 13.

Mirrors M1–M4

Four mirrors are used to remove the rotations produced by azimuth and elevation movements and produce a constant beam in the receiver cabin. M1 is fixed to the primary mirror structure, and M2–M4 to the rotating part of the azimuth bearing. As now envisaged, these are all plane mirrors, for the following reasons:

(1) They are cheaper to fabricate than shaped reflectors;
(2) They are simple to align;

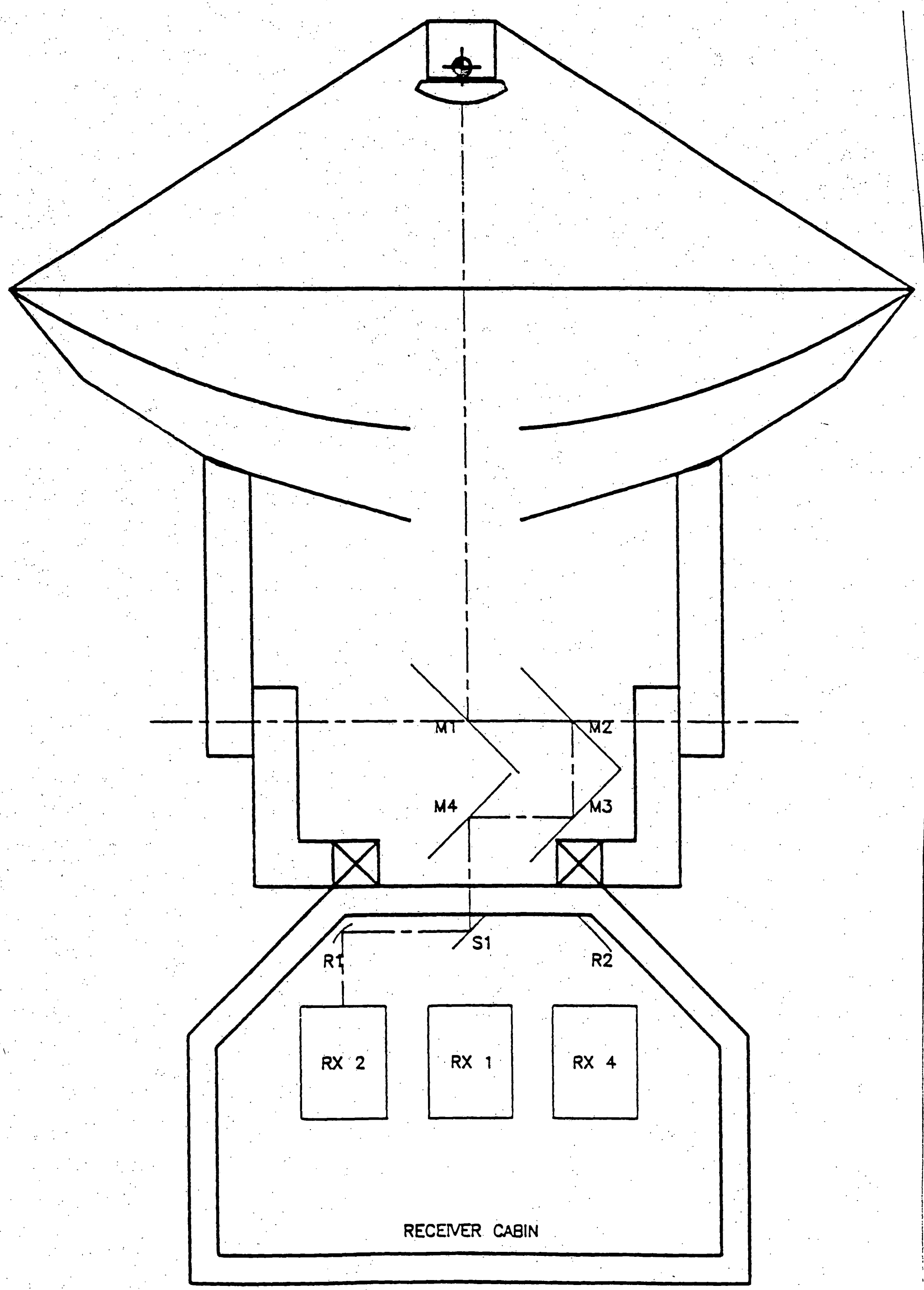

Figure 1. Proposed optics for the MMA antennas.

(3) The imaging properties of shaped mirrors for off-axis beams are unknown.

The sizes of these mirrors vary from about 1.4×0.95 m to 1.0×0.74 m.

Receiver Room

The receiver room is located in the base of the antenna mount. Five receiver bays are planned (Figures 1 and 2). One is in the center of the room and is intended for a focal plane array at frequencies down to about 200 GHz. It receives the signal directly from M4, through the azimuth bearing. Note that the image of the sky rotates relative to this receiver position, so that either the receiver has to be rotated or software correction has to be applied.

For the other receiver positions the beam is deflected by selection mirror S1 to one of the receiver focusing mirrors R1–R4. These receivers may be single beam at any frequency from 43–500 GHz, or possibly an array at the higher frequencies (300 GHz and higher).

The receiver front-ends should be about $0.75 \times 0.75 \times 1.0$ m. Although this is smaller than the receivers on the 12-m telescope, some of the associated electronics can be removed to racks at the side of the receiver room.

Discussion

Table 1 summarizes the main parameters of the design. The specification that the secondary focus be brought to the receiver imposes quite stringent conditions on the geometry and dimensions. The values given here therefore cannot be changed by very much. As far as the telescope performance is concerned, the main consequence is the relatively large central blockage, leading to increased sidelobes and reduced aperture efficiency. The reduction in gain due to the 1-m diameter hole in the primary is about 5.4%. In order to reduce the size of the central blockage significantly, the secondary focus would need to be brought much closer to the vertex, and M1 and M4 (for example) would need to be focusing reflectors. Because of the disadvantages listed earlier, this should be considered only if the blockage is shown to be unacceptable.

Figure 2 gives the main dimensions set by the choice of the optics. Figures 3–5 show how the beams of different receivers couple to the telescope. A Gaussian beam giving an edge taper of 11 dB is assumed, and the 1- and 2-beam radii contours are plotted. The 2- beam radii contours are a fairly conservative estimate of the clearance required, but this should not be reduced, if at all possible.

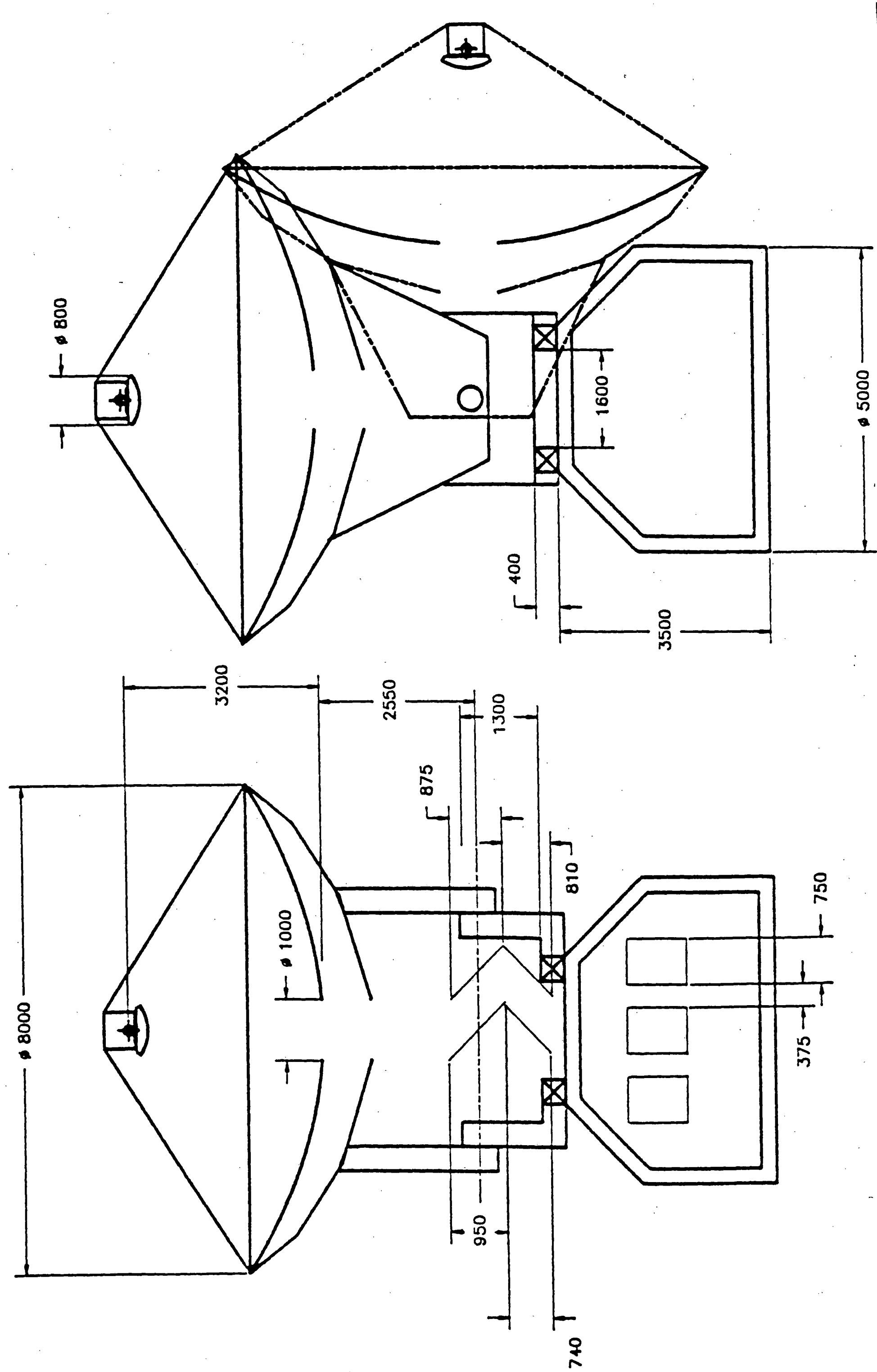

Figure 2. Preliminary choices for dimensions of antenna (in units of millimeters).

Table 1. Principal design parameters.

Primary Mirror —		
Shape		Paraboloidal
Diameter	D	8.00 m
Focal length	f	3.20 m
Focal ratio	f/D	0.4
Edge angle	θ_p	64°.01
Central hole diameter	d_h	1.00 m
Secondary Mirror —		
Shape		Hyperboloidal
Diameter	d_s	0.80 m
Distance f_s between foci	$f_s = 2c$	9.7908 m
Additional path length	$2a$	9.18409 m
Eccentricity	e	1.06897
Magnification	M	30
Paraxial focal length	$f_a = a(e^2 - 1)/2$	0.655 m
Equivalent Paraboloid —		
Focal length	$F = Mf$	96.0 m
Focal ratio	F/D	12.0
Edge angle	$\theta_s = 2\cot^{-1} 4F$	2°.39
Plate scale	$1/F$	2.15 arcsec mm^{-1}

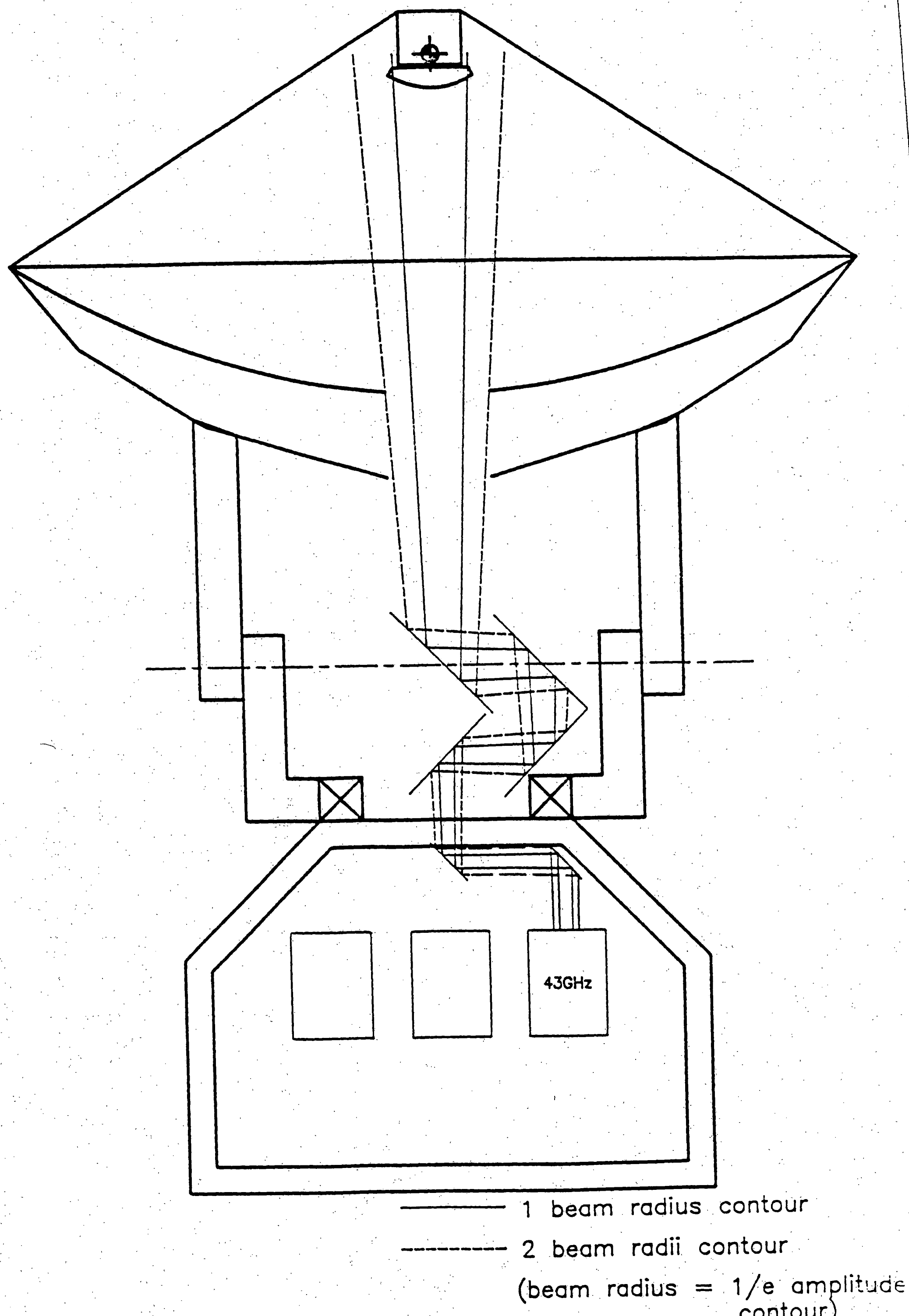

Figure 3. 43 GHz beam path.

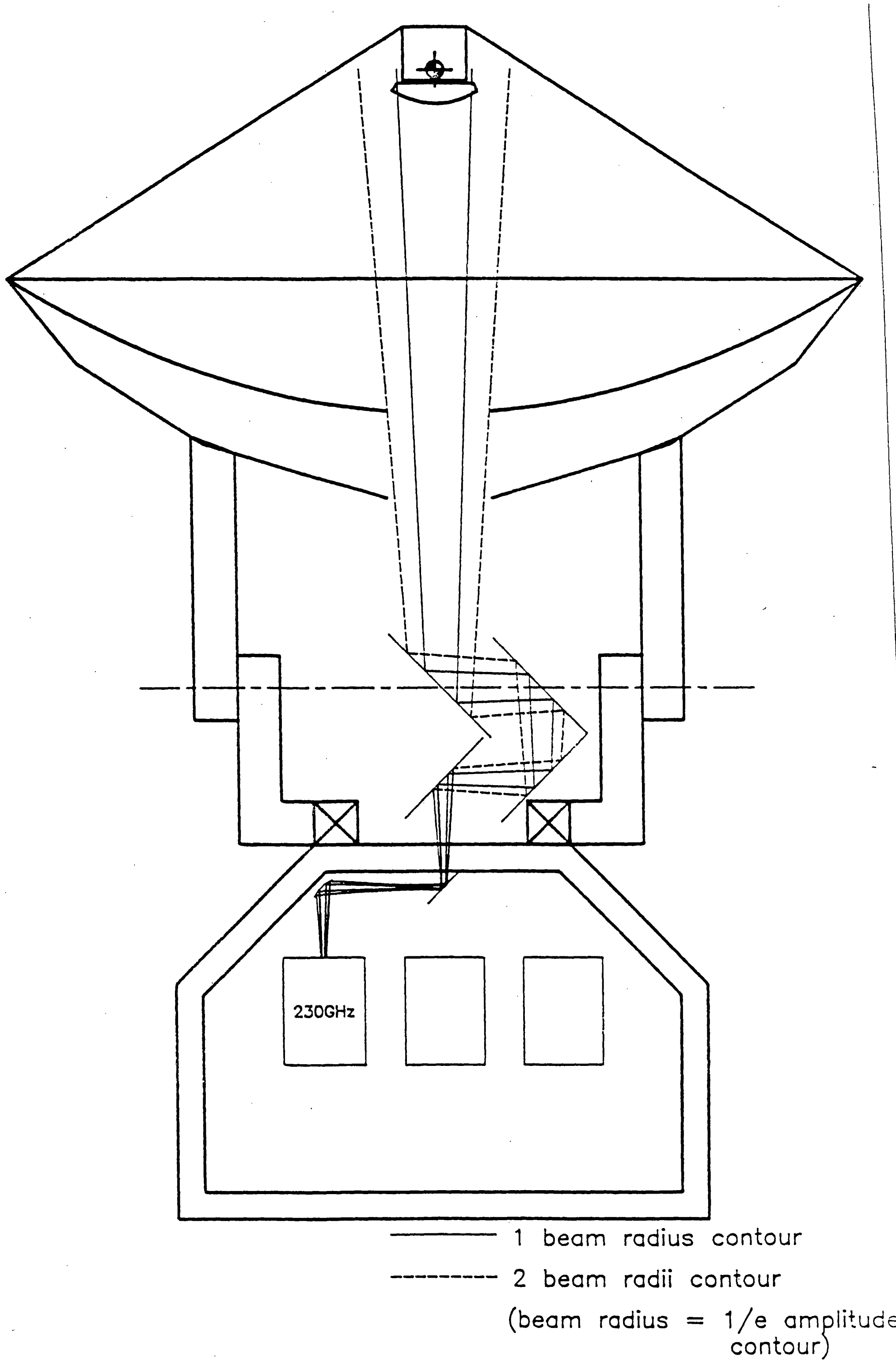

Figure 4. 230 GHz beam path.

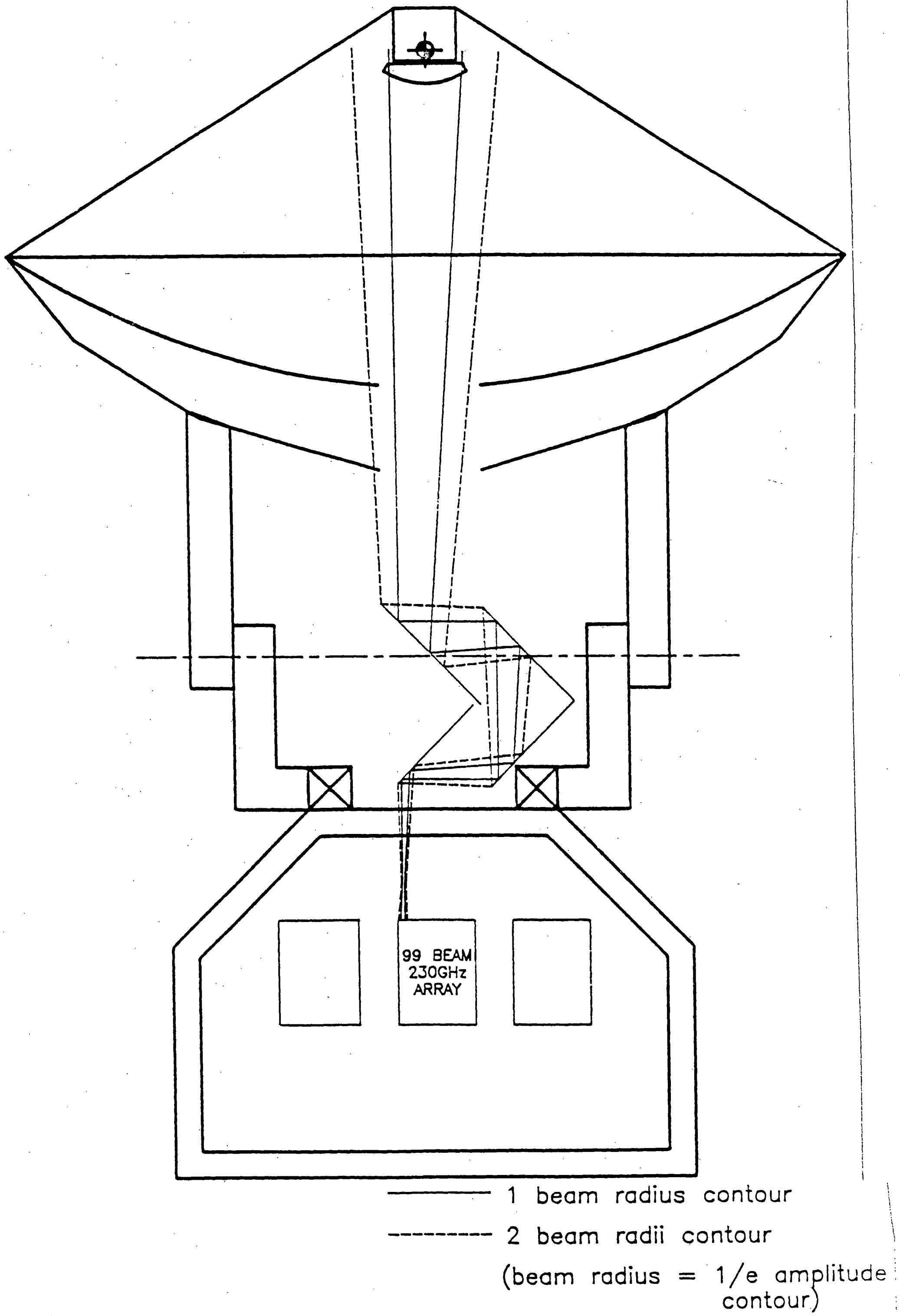

Figure 5. 230 GHz offset beam.

MOSAICING AND THE CENTRAL ELEMENT

One crucial requirement of the MMA is that it should be able to measure essentially all Fourier components relevant to a region of sky, up to the cutoff in maximum spacing of a few kilometers. Particular emphasis must be given the measurement of short-spacing information, because it is crucial for imaging large objects. By 'short', we mean spacings less than or close to the antenna diameter of 7.5 m, say 0–10 meters. In conventional interferometers, these and shorter spacings are often missing completely. However, since the MMA will regularly image objects much larger than an individual primary beam, these spacings are vital. There are three possible schemes for obtaining the measurements:

(1) *Large Single Dish:* This is the most conventional of the schemes. A large single-dish is used to image the sky in total-power mode. The required spacings could be obtained by inverse Fourier transformation of the image followed by correction of the sensitivity function of the dish (i.e., the inverse Fourier transform of the primary beam). According to the conventional wisdom, the size of the single-dish should be 2–3 times *larger* than the required spacings.

(2) *Multi-Telescope Array:* An array of smaller telescopes is used as an interferometric array, and a subset of the required spacings is obtained directly. The size of the elements should be 2–3 times *smaller* than the size of the large array elements. To avoid shadowing between the densely packed elements, the elements should be mounted on a backing structure which can point at and track the object. Structures on the largest scale-size are derived from total-power measurements using the larger interferometer dishes.

(3) *Homogeneous Array:* This is the most radical of the schemes and the one of greatest potential. There would not be a central element: each antenna in the interferometer array would be equipped to observe in a total-power mode, preferably simultaneously with the interferometer measurements. As the array is scanned for mosaicing, the total-power observations can be used to form an image which could be inverse-transformed to obtain spacings up to some fraction of the dish diameter. In principle, this can be generalized for the interferometer elements, and it provides information on scales ranging down from the shortest spacing by some fraction of the dish diameter. Therefore, if the shortest spacing is about a dish diameter, and if the extrapolated measurements are good at offsets of up to half a dish diameter, then there is no gap to be filled.

Some variant of the mosaicing technique would be used in each of the three cases. Although all three options are theoretically feasible, there may be practical difficulties with each. Our current task is to investigate these obstacles and reassess the viability of each option. The main questions can be summarized as follows:

(1) Given perfect observations, will mosaicing allow recovery of all spacings:

 (a) down to about half the dish diameter, from interferometric measurements?

 (b) up to about half the dish diameter, from the total-power measurements?

(2) Will the various instrumental errors corrupt the mosaicing? For example, will pointing errors be a limiting factor? Or reversing the question, what are the necessary specifications on pointing, illumination stability, cross-talk, etc.?

(3) How do observational details affect the design? For example, can we design a homogeneous array which allows sufficient non-shadowed integration time? Beam-switching will be required for total-power measurements—how far a throw is necessary? Can the optics accommodate it?

(4) Are the total-power measurements significantly more difficult than the interferometric measurements? Is a single-feed array with N elements easier to maintain than the feeds on N separate telescopes?

Answers to these questions are difficult to obtain. Mosaicing is a particularly thorny procedure to analyze theoretically since in part it relies on a nonlinear algorithm, MEM, for a crucial step. Consequently, we do not believe that a full theoretical analysis of mosaicing is possible. As an alternative approach, we suggest that many of the issues concerning the central element are best addressed by computer simulations. We also believe that simulations are necessary to settle more general questions about the Millimeter Array design. Since the MMA will be the first radio interferometric array designed for mosaicing, we believe that a demonstration of the array via computer simulation is vital. For these reasons we have developed a simulation package to test mosaicing of complex objects in realistic conditions. The package produces pseudo-data that will allow us to accurately simulate mosaicing observations with the MMA in the presence of atmospheric disturbances, pointing errors, and aperture-illumination errors. It will also be useful for investigating some more general questions about the MMA design; for example: are equatorial mounts for the antennas advantageous? what is the required upper limit on pointing errors? It is planned that the package will be used over the entire design phase of the MMA, although some simple results are already available. These include studies of the effect of incomplete knowledge of the primary beam on the reconstruction of a mosaiced image and of the degradation of such an image by pointing errors in the individual pointings.

Specific results from the simulation program are in hand for the following:

- A demonstration of the imaging properties of the compact config-

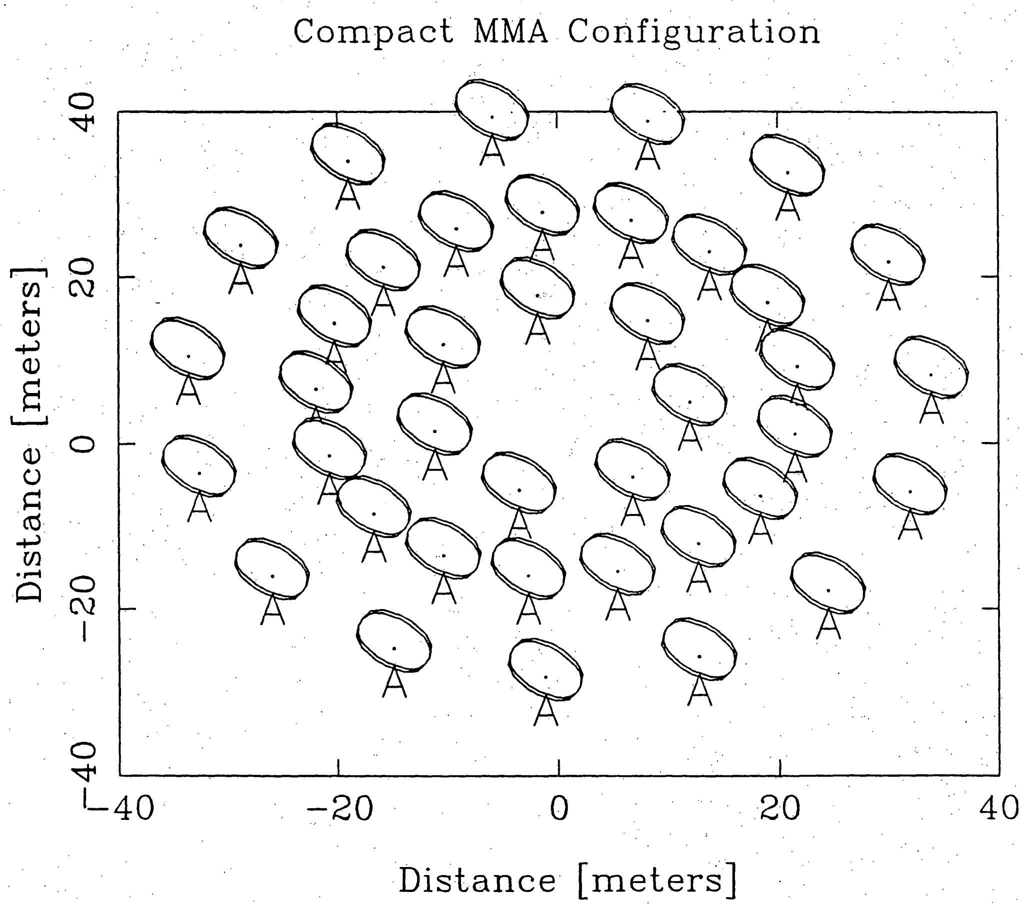

Figure 1. A possible compact configuration of array elements for the MMA.

uration for perfect data. The instantaneous u-v coverage of the compact array shown in Figure 1 is good enough that an excellent 100-pointing mosaic can be obtained in a few hours. A comparison of the MMA simulation with that obtained from the simulation of a representative 9-element array shows the imaging of the MMA to be a significant improvement.

- Investigation of atmospheric models appropriate for the simulations. This covers the relationship between fluctuations in opacity, brightness temperature, and excess path length, as well as the spectrum of the turbulence. We believe that we have a formalism suitable for generating visibility data with reasonably authentic errors.
- Investigation of the effects of truncation of our knowledge of the primary beams of the array elements. The news here is very encouraging: reasonable-quality images can be obtained even when the primary beam is known only down to the 5% contour. This has been investigated only for well-isolated objects; the next step is to

see if it still holds for a mosaic of part of a crowded field. This robustness can be attributed to the redundancy of information in the image plane sampling, and to the deconvolution algorithm used. This does bode well for the future simulations concerning pointing errors and may indicate that we have been overly concerned about the effect of errors in mosaicing.

- A large part of the required software is now in hand, and we are proceeding with further tests, most immediately concerning pointing errors.

The simulations lead us to the tentative conclusion that a large central element seems not to be required: complete short-spacing information can be obtained from a homogeneous array. However, this conclusion is subject to revision as we get even more experience with the simulations.

In addition to the simulations, observational tests are being carried out. The Hat Creek BIMA millimeter array is being used for various tests of mosaicing which should shed some light on a number of topics, including the importance of pointing errors. Tim Cornwell and Robert Braun are planning to test spectral line mosaicing using H I observations of M33 made with the VLA. Here the goal is to make use of the fact that spectral line observations provide the equivalent of the 'zero-spacing' flux from the measured autocorrelations; in principle these can be incorporated into the imaging. Now we wish to investigate the extent to which this works in practice.

The computational resource requirement of mosaicing has already been analyzed in substantial detail and is presented in Chapter V of MMA Design Study Vol. II. There, a rough cost estimate—$4M for all required calibration and imaging hardware (mosaicing requirements are predominant among total needs)—was given; this is still our best estimate. The overall needs of the MMA in off-line computing are essentially the same as those of the VLA; what differs for the MMA is simply the mix (i.e., the way these needs are proportioned) and the total. In addition, the budget for on-line computing hardware was estimated in Vol. II as $2M; on-line needs have still not been considered in detail, but our experience with VLA and VLBI real-time operation makes this analysis relatively straightforward.

RECEIVERS

During the time period since the *Millimeter Array Design Concept* was written, there have been several developments in millimeter wave receivers which may influence our approach to the MMA receivers.

1. Improvement of SIS receiver sensitivity

Through the use of integrated tuning circuits, we have been able to reduce the mixer noise temperature to within a factor of two of the photon noise $\hbar\omega/k_B$ in SIS mixers for the 3-mm band [1]. At 115 GHz, with $T_{\rm mixer} \leq 5.6$ K DSB, the receiver noise temperature referred to the mixer input flange in our laboratory test receiver is $\leq$ 9.5 K DSB. Allowing for window losses in a well-designed telescope receiver, it should be possible to achieve $T_{\rm rcvr} < 20$ K DSB, measured at the dewar input.

2. An SIS receiver with no adjustable tuners

An experimental fully-integrated 3-mm SIS mixer has given promising results over 70–115 GHz (a 49% bandwidth) without any tuning adjustments [2]. The receiver noise temperatures plotted in Figure 1 are referred to the input flange of the mixer. We have not yet investigated the saturation (dynamic range) characteristics or sideband ratio of this mixer.

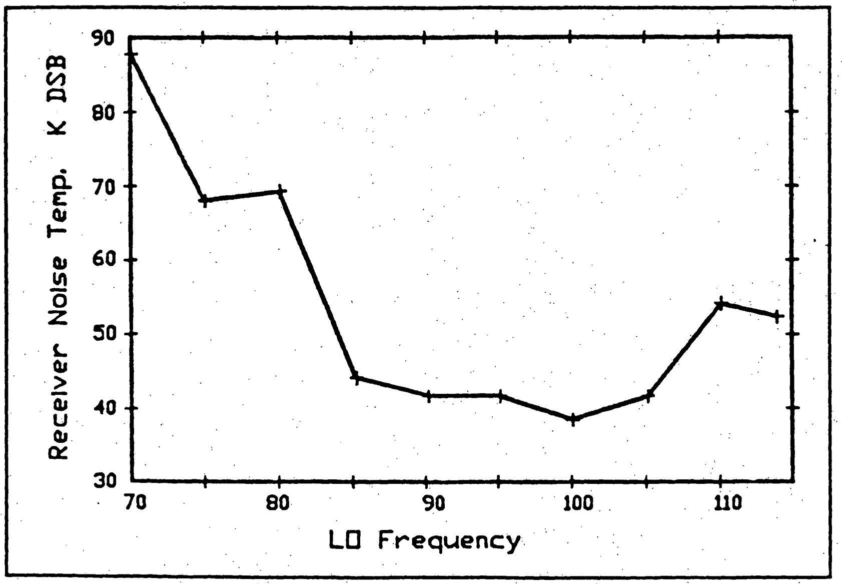

Figure 1. Noise temperature, referred to the mixer input flange, of an SIS receiver using an experimental fully-integrated mixer with no adjustable tuners [2].

3. Planar log-spiral mixer

Caltech results for an SIS junction mounted at the vertex of a planar log-spiral antenna on a quartz substrate [3] have excited considerable interest in the radio astronomy community. Reported receiver noise temperatures are plotted in Figure 2. At the lower frequencies the receiver was driven into saturation by thermal radiation from a room-temperature black-body; this is not surprising as the thermal radiation in a 500 GHz bandwidth at 300 K is about 2 nW, which is of the same order as the LO power required by a single-junction SIS mixer at 100 GHz. Series arrays of junctions and integrated tuning circuits may eventually enable this type of mixer to be used to advantage on the MMA.

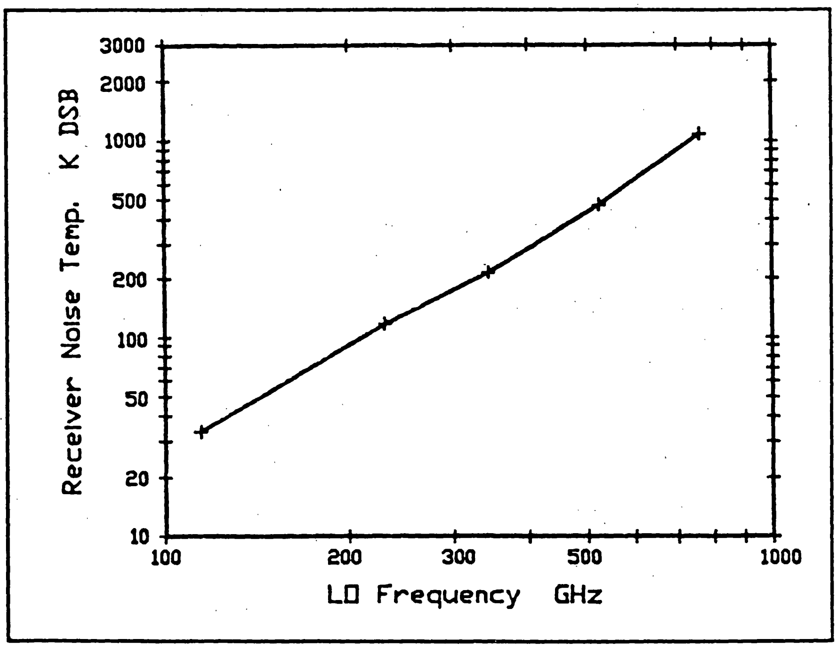

Figure 2. Noise temperature of an SIS receiver using a planar log-spiral mixer [3].

4. Improvement in SIS junction quality

Work at UVa under NRAO contract has made good progress. They have recently made Nb/Al-Al_2O_3/Nb SIS junctions with the highest quality parameter ($V_{\text{mixer}} = 1400$ mV) ever reported, and NbN/Ox/PbBi edge junctions with the highest V_{mixer} and gap voltage ever reported for edge junctions. These two SIS technologies may well end up as the prime choices for low-noise millimeter and submillimeter heterodyne receivers. At present the UVa group is in a precarious financial state, largely as a result of their loss of support from NASA and JPL. Unless substantial additional support is found soon, they will be forced to terminate their work on SIS devices. Such an occurrence would represent a serious loss to this country of unique technology and expertise.

5. Local oscillators

The local oscillators for the MMA will almost certainly be varactor-diode frequency multipliers driven by phase-locked Gunn oscillators. Commercial development of InP Gunn diodes is continuing, but development of very widely tunable (25–40% for the MMA) oscillators using those diodes will almost certainly need to be undertaken as part of the MMA project. Possibly, two LO's will be needed per MMA frequency band.

Reliable, widely tunable frequency multipliers will need to be developed. Very high-quality planar (i.e., whiskerless) Schottky mixer diodes have recently been made at UVa [4]. With suitable modification these should be well-suited to multiplier operation. Unfortunately, budgetary considerations have forced NRAO to discontinue its support for all Schottky diode work at UVa.

Recent work at Caltech on planar grids of varactor diodes has demonstrated high efficiency multiplication at millimeter wavelengths [5]. An efficiency of 9.5% has been achieved experimentally in doubling to 66 GHz, and it is anticipated that 30% efficiency should eventually be possible in doubling to $\sim$ 200 GHz. These designs are for input powers of many watts, and it is not clear whether they could be suitably scaled for operation at the milliwatt level available from Gunn oscillators.

References

[1] S.-K. Pan, A. R. Kerr, M. J. Feldman, A. Kleinsasser, J. Stasiak, R. L. Sandstrom, and W. J. Gallagher, "An 85-116 GHz SIS receiver using inductively shunted edge-junctions", *IEEE Trans. Microwave Theory Tech.*, Vol. **MTT-37**, No. 3, Mar. 1989.

[2] A. R. Kerr and S.-K. Pan, NRAO. Private communication.

[3] T. H. Büttgenbach, R. E. Miller, M. J. Wengler, D. M. Watson, and T. G. Phillips, "A broadband low noise SIS receiver for submillimeter astronomy", *IEEE International Microwave Symposium, Digest of Technical Papers*, June 1988, pp. 469–472.

[4] D. G. Garfield, R. J. Mattauch, and W. L. Bishop, "Design, fabrication, and testing of a novel planar Schottky barrier diode for millimeter and submillimeter wavelengths", *Proc. IEEE Southeastcon '88*, April 1988, pp. 154–160.

[5] C. F. Jou, W. W. Lam, H. Z. Chen, K. S. Stolt, N. C. Luhmann, and D. B. Rutledge, "Millimeter-wave diode-grid frequency doubler", *IEEE Trans. Microwave Theory Tech.*, Vol. **MTT-36**, No. 11, Nov. 1988, pp. 1507–1514.

CORRELATOR

The correlator design for the Millimeter Array is still in a rudimentary state. It consists of the concept given in Design Study Volume II [1], along with some refinements to the cost equation and its parameters given in a memo by D'Addario [2]. In February 1988, the Advisory Committee recommended [3] that "flexibility" be a major design goal of the correlator, with particular emphasis on being able to separate the sidebands of a DSB front end and on being able to observe more than one line at a time. Here we attempt to address these and other flexibility issues.

1. Assumptions

As a starting point, consider a correlator that accepts 2 GHz of signal bandwidth from each of 40 antennas and computes the complex cross-power spectrum on each baseline with a frequency resolution of 2 MHz. This is the machine whose cost we attempted to estimate in the earlier documents; let it be called the "nominal" correlator. The cost is still very uncertain, being a strong function of rapidly changing technology.

Little has been said about the organization of the signals or about the various possible modes of operation. Here we assume that:

(a) The 2 GHz bandwidth is supplied in $J \geq 4$ separate channels, and these can be processed independently by the correlator. The channels may be from different front ends, from different parts of a wide IF in one front end, from different polarizations, or some combination of these.

(b) Fringe stopping has been done in the LOs. This means that the fringes have been stopped at the total LO frequency for each channel or at the center frequency of the channel.

(c) The front ends use double-sideband mixers, but accurate phase switching of the first LO in increments of $\pi/2$ is possible, and this can be synchronized with correlator integrations.

2. Options

Separation of Sidebands. Given the assumption that accurate phase-switching of the first LO is available, visibilities in each sideband can be measured separately. If the switching interval is not too short, then this requires doubling the size of only the long-term accumulator in the correlator. The long-term accumulator is usually less than 10% of the cost of the cross-correlation part of the correlator. If the short-term dump time of the correlator is 100 msec, then for 40 antennas the total switching cycle time would be 6.4 sec (assuming Walsh function switching patterns), which becomes the quantum of integrating time for sideband-separated observations.

The sideband separation does not in itself impose any penalty in signal-to-noise ratio (SNR); that is, a line appearing in only one sideband will be detected with the same SNR whether or not the sideband separation procedure is applied. But the noise of both sidebands is present in each result, so the SNR is worse than if the front ends had been single-sideband, typically by a factor of $\sqrt{2}$.

Polarization. For polarization measurements, the nominal correlator can be re-organized to produce the necessary cross-polarized correlations provided that only half the maximum bandwidth is processed. That is, if half of the input channels are unused then the corresponding sections of the correlator can be devoted to the additional correlations. This is possible in either the FX or XF architecture. The cost lies in providing the appropriate interconnections between correlator sections; in accord with our experience in designing the VLA and VLBA correlators, the incremental cost can be made negligible by careful design. On the other hand, if full polarization measurements must be made at the full bandwidth, then the cost of the *cross-correlation part* of the correlator must be doubled. With present technology, it appears that the cross-correlation part dominates the cost in any architecture, in which case the total cost also doubles.

In the XF case, it is also possible to obtain polarization measurements by degrading the spectral resolution while continuing to process the full bandwidth. This does not work with an FX correlator.

Multiple Observing Bands or Lines. This has a bigger effect on the design of the front ends and IF processing than on the correlator. The question is to what extent the correlator input channels are separately tunable. We have assumed that a minimum of 4 channels is available, and for various reasons 8 or 16 channels may be more appropriate. It is straightforward to arrange that each channel may be tuned to any frequency within the bandwidth of the first IF; in addition, any available front end can be connected to any channel.

It may be desirable to operate different channels at different resolution or bandwidth. This will be possible if the correlator is organized as J quasi-independent correlators, each handling one channel of all N antennas. Such an organization also facilitates a future increase in J by adding identical hardware, but makes difficult a future increase in N.

High Resolution. The maximum bandwidth of each channel is B/J, where B is the total bandwidth (assumed to be 2 GHz) and J is the number of channels. If the channel bandwidth is reduced by filtering, then the resolution can be decreased by recirculation. This applies to either the FX or XF architecture, but in the FX case the additional memory must be built into every stage of the FFT engine and the number of stages must be increased by $\log_R \alpha$ where α is the bandwidth reduction factor and R is the FFT radix. In any case, the resolution becomes b/α^2. The same is true if the total bandwidth is reduced by not using some channels, keeping the bandwidth of each channel the same, provided that the cross-correlation hardware of the unused channels can be re-allocated.

The FX correlator is at a disadvantage because it must be built for a particular maximum FFT length. The VLBA correlator has a degree of freedom not available here, namely variation of the tape speed to keep the correlator input bandwidth constant while varying the observing bandwidth.

Trading Baselines for Bandwidth or Resolution. If each antenna actually provides more channels than the correlator can process, then by not using some antennas and connecting the extra channels from the remaining antennas to the now-free correlator inputs, larger bandwidth can be accepted. This would be useful only for special purposes, such as observing more lines simultaneously when SNR and u-v coverage on any one line is not a limitation.

Another such trade is conceivable. While retaining all antennas at the full bandwidth, some baselines might be of little interest because of redundant u-v coverage. In principle, the cross-correlation hardware for these baselines might be re-allocated to improve the spectral resolution on the other baselines. However, this increases the complexity of correlator organization to such an extent that it should not be implemented unless a strong case is made for its importance.

References

[1] *The Millimeter Array Design Concept*, Millimeter Array Design Study Volume II, Section VI.4, NRAO, Jan. 1988.

[2] L. R. D'Addario, "Millimeter Array Correlator Cost Equation", February 1988.

[3] R. L. Brown, "Millimeter Array Advisory Committee Suggestions", April 13, 1988.